COHERENT AND INCOHERENT DYNAMICS IN A PERIODICALLY DRIVEN BISTABLE SYSTEM

T. DITTRICH, F. GROSSMANN, P. HÄNGGI, B. OELSCHLÄGEL and R. UTERMANN
Institut für Physik, Universität Augsburg,
Memminger Straße 6, D-86135 Augsburg, Germany

Abstract. We study the conservative as well as the dissipative quantal dynamics in a harmonically driven, quartic double-well potential. Our main tool is a numerical analysis of time evolution and spectrum, based on the Floquet formalism. In the deep quantal regime, we find coherent modifications of tunneling, including its complete suppression. In the semiclassical regime of the conservative system, the dynamics is dominated by the competition of tunneling between symmetry-related regular regions and chaotic diffusion along the separatrix. We demonstrate that there is a strong correlation between each tunnel splitting and the overlap of the associated doublet states with the chaotic layer. In the dissipative case, remnants of coherent behavior occur as transients, such as the tunneling between distinct, coexisting limit cycles. In particular, the coherent suppression of tunneling is stabilized by weak incoherence. The quantal stationary states are characterized by an anisotropical broadening due to quantum noise, as compared to the corresponding classical attractors.

1. Introduction

A good way to learn about the interplay of coherent and incoherent dynamics, of stochasticity and deterministic chaos is to study specific systems where they occur simultaneously. Bistable systems form an important paradigm: They contain the essence of a wealth of nonlinear phenomena, from the microscopic to the macroscopic realm [1 – 5]. With a periodic driving added, their classical repertoire of behavior ranges from limit cycles to several coexisting strange attractors [6 – 9]. On the quantum-mechanical level, bistable systems provide the standard example of coherent tunneling [10].

In the present paper we investigate the nature of the transition from the simple coherent quantal dynamics to the intricate complexity of the macroscopic behavior, focussing on a few selected landmarks. This transition has two basic aspects: One of them is the sheer increase in system size. In the formal description, it is reflected in an increase of characteristic actions, compared to $\hbar$, and thus corresponds to the short-wavelength or semiclassical limit. The other aspect is the growing importance of ambient and internal degrees of freedom, weakly coupled to the system in focus, and usually modelled collectively as a reservoir.

The transition to short characteristic wavelengths lets classical phase-space structures emerge more and more clearly in the quantal dynamics. Specifically, in the case of bistable systems, we shall ask how the onset of chaos on the classical level

becomes manifest in the tunneling.

Incoherent processes induced by the ambient degrees of freedom, in turn, tend to smooth out the fine interference patterns in phase space and time which encode classical behavior on the quantal level, and thus render the semiclassical limit less singular. We study the stationary states approached by the dissipative quantum system—they correspond to the attractors of the classical flow—and the decay of coherence in the transient behavior preceeding them.

We shall introduce our working model, the harmonically driven quartic double well, and its symmetries in Section 2. Section 3 is devoted to the modifications of tunneling, due to the driving, in the deep quantal regime. In Section 4, we discuss driven tunneling in the semiclassical regime where it begins to exhibit the influence of classical chaos. The consequences of incoherent processes, of damping and noise, are addressed in Section 5. Section 6 summarizes our survey of coherent and incoherent behavior in bistable systems.

The present work forms a synopsis of results partially published elsewhere [11 – 19].

2. The model and its symmetries

The harmonically driven quartic double well is described by the Hamiltonian

$$H_{\mathrm{DW}}(x,p;t) = H_0 + H_1, \quad H_0(x,p) = \frac{p^2}{2} - \frac{1}{4}x^2 + \frac{1}{64D}x^4, \; H_1(x;t) = x\,S\cos\omega t. \tag{1}$$

With the dimensionless variables used, the only parameter controlling the unperturbed Hamiltonian $H_0(x,p)$ is the barrier height D. It can also be interpreted as the (approximate) number of doublets with energies below the top of the barrier. Accordingly, the classical limit amounts to letting $D \to \infty$. The driving is characterized by its amplitude S and frequency ω.

The symmetry of the Hamiltonian under discrete time translations, $t \to t + 2\pi/\omega$, enables to use the Floquet formalism [20 – 23], which generalizes most of the conceptual tools of spectral analysis to the present context. Its basic ingredient is the Floquet operator, i.e., the unitary propagator that generates the time evolution over one period of the driving force,

$$U = \mathsf{T}\exp\left(-\frac{\mathrm{i}}{\hbar}\int_0^{2\pi/\omega} \mathrm{d}t\, H_{\mathrm{DW}}(t)\right), \tag{2}$$

where T effects time ordering. Its eigenvectors and eigenphases, referred to as *Floquet states* and *quasienergies*, respectively, can be written in the form

$$|\,\psi_\alpha(t)\,\rangle = \mathrm{e}^{-\mathrm{i}\epsilon_\alpha t}|\,\phi_\alpha(t)\,\rangle, \text{ with } |\,\phi_\alpha(t+2\pi/\omega)\,\rangle = |\,\phi_\alpha(t)\,\rangle. \tag{3}$$

From a Fourier expansion of the $|\,\phi_\alpha(t)\,\rangle$,

$$|\,\phi_\alpha(t)\,\rangle = \sum_k |\,\phi_{\alpha,k}\,\rangle \mathrm{e}^{-\mathrm{i}k\omega t}, \quad |\,\phi_{\alpha,k}\,\rangle = \frac{\omega}{2\pi}\int_0^{2\pi/\omega} \mathrm{d}t\,|\,\phi_\alpha(t)\,\rangle \mathrm{e}^{\mathrm{i}k\omega t}, \tag{4}$$

it is obvious that the quasienergies are organized in classes, $\epsilon_{\alpha,k} = \epsilon_\alpha + k\omega$, $k = 0, \pm 1, \pm 2, \ldots$, where each member corresponds to a physically equivalent solution. Therefore, all spectral information is contained in a single "Brillouin zone", $-\omega/2 \leq \epsilon < \omega/2$.

Besides invariance under time translation and time reversal, the unperturbed system possesses the spatial reflection symmetry $x \to -x$, $p \to p$, $t \to t$. For a general driving, this symmetry is destroyed. For the specific time dependence of a harmonic driving, however, the symmetry $f(t + \pi/\omega) = -f(t)$ restores a similar situation as in the unperturbed case: The system is now invariant against the operation [11 – 13, 24]

$$\mathsf{P} : p \to -p, \quad x \to -x, \quad t \to t + \frac{\pi}{\omega}, \tag{5}$$

which may be regarded as a *generalized parity* in the extended phase space spanned by x, p, and phase, i.e., time $t \bmod(2\pi/\omega)$. As in the unperturbed case, this enables to separate the eigenstates into an even and an odd subset.

3. Driven tunneling and localization

To give an impression of driven tunneling in the deep quantal regime, we study in the following how a state, prepared as a coherent state centered in the left well, evolves in time under the external force. Since this state is approximately given by a superposition of the two lowest unperturbed eigenstates, $|\Phi(0)\rangle \approx (|\Psi_1\rangle + |\Psi_2\rangle)/\sqrt{2}$, its time evolution is dominated by the Floquet-state doublet originating from $|\Psi_1\rangle$ and $|\Psi_2\rangle$, and the splitting $\epsilon_2 - \epsilon_1$ of its quasienergies.

There are two regimes in the (ω, S)-plane where tunneling is not qualitatively altered by the external force: Both in the limits of slow (adiabatic) and of fast driving, the separation of the time scales of the inherent dynamics and of the external force effectively uncouples these two processes and results in a mere renormalization of the tunnel splitting Δ. Specifically, as both an analytical treatment and numerical experiments show, the driving always reduces the effective barrier height and thus increases the tunneling rate in these two limits [11].

Qualitative changes in the tunneling behavior are expected as soon as the driving frequency becomes comparable to the internal frequencies of the double well, in particular, to the tunnel splitting and to the so-called resonances $E_3 - E_2$, $E_4 - E_1$, $E_5 - E_2$, ... By spectral decomposition, the temporal complexity in this regime is immediately related to the "landscape" of quasienergy planes $\epsilon_{\alpha,k}(\omega, S)$ in parameter space. Features of particular significance are close encounters of quasienergies: Two quasienergies cross one another without disturbance if they belong to different parity classes, otherwise they form an avoided crossing.

A quantity well suited to study the relationship between dynamics and quasienergy spectrum is the *probability to return* [25, 26],

$$P^\Phi(t_n) = |\langle \Phi(0) \,|\, \Phi(t_n) \rangle|^2 = |\langle \Phi(0) \,|\, U^n \,|\, \Phi(0) \rangle|^2, \quad t_n = \frac{2\pi n}{\omega}, \; n = 0, \pm 1, \pm 2, \ldots, \tag{6}$$

defined with respect to some initial state $|\Phi(0)\rangle$, and with time restricted to the instances of zero phase of the driving. By expanding $P^\Phi(t_n)$ in the basis provided

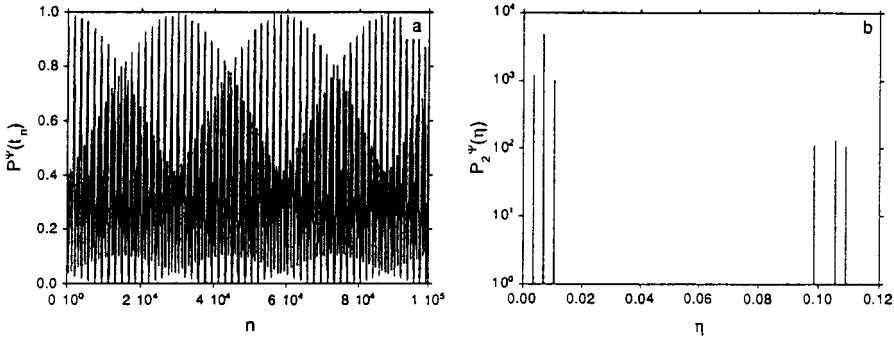

Fig. 1. Driven tunneling at the fundamental resonance $\omega = E_3 - E_2$. (a) Time evolution of $P^{\Phi}(t_n)$ over the first 2×10^5 time steps; (b) local spectral two-point correlation function $P_2^{\Phi}(\eta)$ obtained from (a). The parameter values are $D = 2$, $S = 2 \times 10^{-3}$, and $\omega = 0.876$.

by the quasienergy eigenstates,

$$P^{\Phi}(t_n) = \xi^{-1} + \sum_{\alpha \neq \beta} \exp[\mathrm{i}(\epsilon_\alpha - \epsilon_\beta)t_n]\, |\langle \phi_\alpha(0) \,|\, \Phi(0) \rangle|^2\, |\langle \phi_\beta(0) \,|\, \Phi(0) \rangle|^2, \quad (7)$$

the rôle of the quasienergies for the time evolution becomes explicit. Here, ξ^{-1} stands for the time-independent diagonal part excluded from the double sum in Eq. (7). It gives the long-time average of $P^{\Phi}(t_n)$. The Fourier transform $P_2^{\Phi}(\eta)$ of the probability to return is the two-point correlation function of the *local* quasienergy spectrum, i.e., the spectrum weighted according to the relative significance of each quasienergy for the specific dynamics starting from $|\Phi(0)\rangle$. Below, we use these concepts to discuss driven tunneling at two parameter points, one of them featuring an avoided quasienergy crossing, the other an exact one [11 - 14].

The "single-photon transition" at $\omega = E_3 - E_2$ is called *fundamental resonance*. At $S = 0$, it is reflected in a crossing between the quasienergies $\epsilon_{2,k}$ and $\epsilon_{3,k-1}$. For $S > 0$, it becomes an avoided crossing, since the corresponding eigenstates have equal parity. Fig. 1a shows the time evolution of $P^{\Phi}(t_n)$ at the fundamental resonance ($D = 2$, $S = 2 \times 10^{-3}$, $\omega = 0.876$). The monochromatic oscillation of $P^{\Phi}(t_n)$ characteristic of unperturbed tunneling has given way to a more complex beat pattern. The Fourier transform of $P^{\Phi}(t_n)$ reveals that these beats are composed mainly of two groups of three frequencies each (Fig. 1b), which can be identified, in turn, as the quasienergy differences $\epsilon_{3,-1} - \epsilon_{2,0}$, $\epsilon_{2,0} - \epsilon_{1,0}$, $\epsilon_{3,-1} - \epsilon_{1,0}$, and $\epsilon_{4,-1} - \epsilon_{3,-1}$, $\epsilon_{4,-1} - \epsilon_{2,0}$, $\epsilon_{4,-1} - \epsilon_{1,0}$, at the avoided crossing.

In contrast, a two-photon transition that bridges the tunnel splitting Δ is "parity forbidden", and thus the quasienergies $\epsilon_{2,k-1}$ and $\epsilon_{1,k+1}$ form an exact crossing. Eq. (7) indicates that a vanishing of the difference $\epsilon_{2,-1} - \epsilon_{1,1}$ will have a remarkable consequence: For a state prepared as an exact superposition of the corresponding two Floquet eigenstates only, $P^{\Phi}(t)$ and all other observables become constants, at least at the discrete times t_n, and thus it is possible that tunneling comes to a standstill! According to an argument going back to von Neumann and Wigner [27, 28], exact crossings should occur along one-dimensional manifolds in the (ω, S)

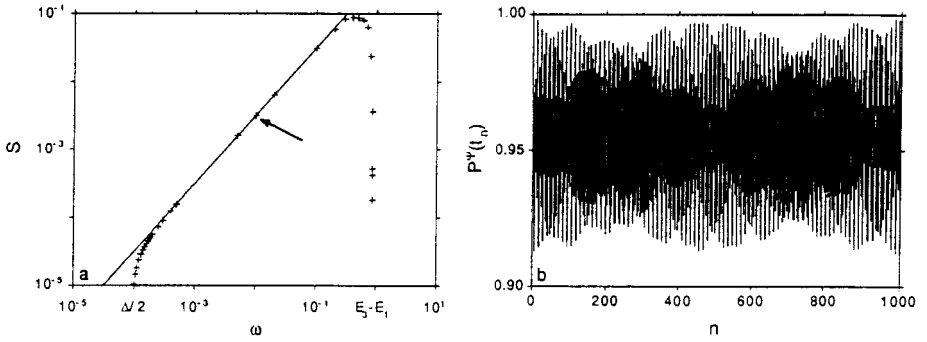

Fig. 2. Suppression of tunneling at an exact crossing $\epsilon_{2,-1} = \epsilon_{1,1}$. (a) The manifold $S_{\mathrm{loc},0}(\omega)$ in the (ω, S) plane where this crossing occurs (data obtained by diagonalization of the full Floquet operator for the driven double well are indicated by crosses, the full line has been derived from a two-state approximation [15, 29], the arrow indicates the parameter point to which part (b) refers); (b) time evolution of $P^{\Phi}(t_n)$ over the first 10^3 time steps.

plane. In the present case, there is one such manifolds $S_{\mathrm{loc},k}(\omega)$ for each condition $\epsilon_{2,-k} = \epsilon_{1,k}$. Fig. 2a shows $S_{\mathrm{loc},0}(\omega)$: It is a closed curve, reflection-symmetric with respect to the line $S = 0$, with an approximately linear frequency dependence for $\Delta \lesssim \omega \lesssim E_3 - E_2$. A typical time evolution of $P^{\Phi}(t_n)$ for a parameter point ($D = 2$, $S = 3.171 \times 10^{-3}$, $\omega = 0.01$) on the linear part of that manifold is presented in Fig. 2b. It clearly indicates that tunneling is almost completely suppressed. The remaining oscillations of small amplitude can be ascribed to an admixture of higher-lying quasienergy states to the initial state. An additional time dependence faster than the driving—it would not show up in a stroboscopic plot like Fig. 2b—does indeed exist, but with an amplitude comparable to that appearing in Fig. 2b (not shown, see refs. [11 - 14].

The suppression of tunneling is an elementary quantum-interference effect. In fact, much of it can be understood on basis of a two-state approximation [15, 29]. It is achieved by solving the equations of motion for the expansion coefficients of a localized initial state in the Hilbert space spanned by the unperturbed ground-state doublet $|\Psi_1\rangle$, $|\Psi_2\rangle$. The two-state approximation yields an analytical expression for each $S_{\mathrm{loc},k}(\omega)$.

4. Tunnel splittings and the onset of chaos

In the classical double well, the most significant consequence of the periodic driving is the onset of deterministic chaos [30], see Fig. 3. It develops around the hyperbolic fixed point at the top of the barrier: As the perturbation is switched on, the stable and the unstable manifold intersecting at this fixed point start to fold and form a homoclinic tangle [31], which extends all along the two lobes of the separatrix and forms a narrow layer of chaotic motion. With S increasing further, this chaotic layer grows in width, at the expense of the two regular zones within the wells, so that the deterministic diffusion between the wells becomes a significant contribution to

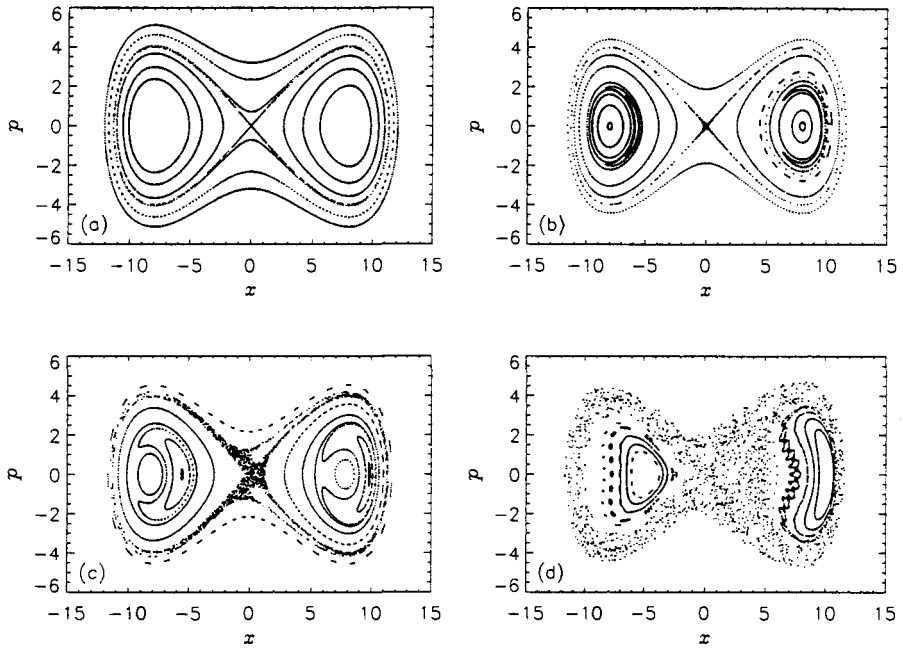

Fig. 3. Classical phase-space portraits of the periodically driven double well at phase 0 of the driving, for various values of the driving amplitude. The parameter values are $D = 8$, $\omega = 0.95$, and (a) $S = 0$, (b) $S = 10^{-3}$, (c) $S = 10^{-2}$, (d) $S = 0.2$.

the classical phase-space transport. There is another conspicuous modification of the phase-space structure, the growth of the regular zone generated by the first resonance of the driving with the unperturbed oscillation [30], which does not, however, affect the coherent dynamics as substantially as the onset of chaos does.

Quantum mechanically, phase-space transport by chaotic diffusion competes with tunneling [32 – 37]. In the present section we investigate how these two processes influence each other. Applying ideas from Einstein-Brillouin-Keller (EBK) quantization for periodically driven systems [38], as well as from random-matrix theory for mixed (regular and chaotic) systems [39], to the present context, we arrive at the following simple expectation [33 – 35]: Even with the driving, the two isolated regular regions within the wells remain related by a discrete symmetry, the generalized parity P (see Eq. 5). Accordingly, Floquet states residing within these regions should form a more or less regular ladder of tunnel-splitted doublets. For states mainly residing within the chaotic layer, in contrast, random-matrix theory predicts level repulsion. We therefore expect that, as soon as one of the pairs of quantizing tori pertaining to the symmetry-related regular regions resolves in the spreading chaotic layer, the exponentially small splitting of the corresponding doublet widens until it reaches a size of the order of the mean level separation. As a consequence, the coherent tunneling on an extremely long time scale will give way to a more irregular

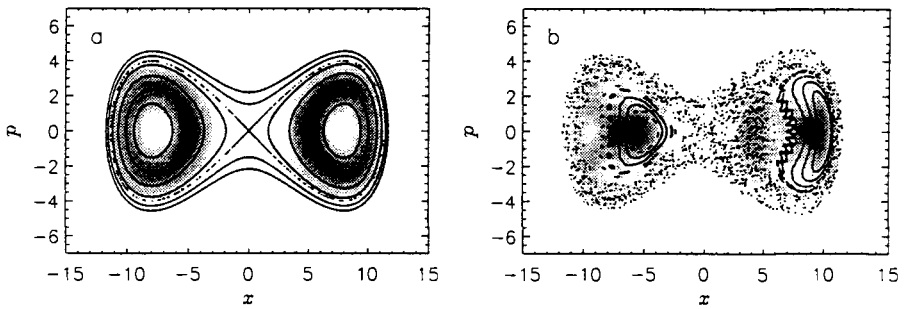

Fig. 4. Husimi distributions (in gray-scale representation) for the quasienergy state $|\phi_7(0)\rangle$, compared with the corresponding classical phase-space portraits, at (a) $S = 10^{-5}$ and (b) $S = 0.2$.

dynamics on shorter time scales, forming the quantal counterpart of deterministic diffusion along the separatrix.

We emphasize that the breakup of the tunnel doublets in the chaotic layer is not a direct consequence of a local property, the positive Lyapunov exponent. Rather, it depends on the fact that diffusive spreading connects all parts of the chaotic layer, even across the symmetry plane. Furthermore, one should keep in mind that the disintegration of a classical torus, looked at closely, is not an abrupt event but proceeds through an intermediate "leaky" stage with fractal dimension ("cantorus") [40]. Even after the cantorus has disappeared, a distinct repelling structure remains within the chaotic layer ("vague torus") [41].

In order to check our hypothesis numerically, we have to quantify the distinction between "regular" and "chaotic" eigenstates, i.e., states located mainly in regions of a corresponding nature in classical phase space. We base this quantification on a quantum-mechanical probability density in phase space, the Husimi distribution [42, 43]. The overlap of the Husimi representation $Q_\alpha(x,p;t)$ of a Floquet state $|\psi_\alpha(t)\rangle$ with the chaotic layer [18, 19],

$$\bar{\Gamma}_\alpha = \frac{\omega}{2\pi}\int_0^{2\pi/\omega} \mathrm{d}t \int_{-\infty}^{\infty} \mathrm{d}x \int_{-\infty}^{\infty} \mathrm{d}p\, Q_\alpha(x,p;t)\Gamma(x,p;t), \tag{8}$$

can be used as a measure of "how chaotic that state is". Here, $\Gamma(x,p;t)$ denotes the characteristic function for the chaotic region. It can be determined numerically, e.g., by letting a trajectory started anywhere in this chaotic region "tick" boxes in a coarse-grained phase space of the desired resolution. Since the Husimi distribution forms a normalized probability distribution over phase space, we have $0 \le \bar{\Gamma}_\alpha \le 1$. As an illustration of these concepts, we compare, in Fig. 4, the Husimi distribution for the quasienergy state $|\phi_7\rangle$ with the corresponding classical phase space portrait, for (a) $S = 10^{-5}$ and for (b) $S = 0.2$, at phase 0 of the driving.

The simple picture sketched above clearly implies a strong relationship between the tunnel splittings $\Delta_\lambda = |\epsilon_{2\lambda,k} - \epsilon_{2\lambda-1,k}|$ and the overlaps $\bar{\Gamma}_{2\lambda-1} \approx \bar{\Gamma}_{2\lambda}$. In Fig. 5, we compare the S dependences of these two sets of quantities for the seven quasienergy doublets from $|\phi_1\rangle$, $|\phi_2\rangle$ to $|\phi_{13}\rangle$, $|\phi_{14}\rangle$ [18, 19]. Qualitatively, we

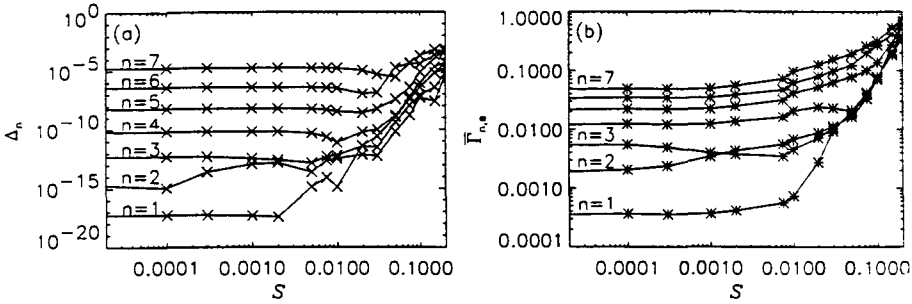

Fig. 5. Tunnel splittings (a) and overlaps with the chaotic layer (b) for the seven lowest tunnel doublets, as functions of the amplitude of the driving.

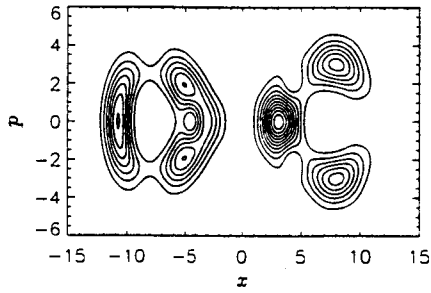

Fig. 6. Contour plot of the Husimi distribution for the quasienergy state $|\phi_{13}(0)\rangle$, at $S = 0.2$.

observe a striking similarity: There is only a weak S dependence, reflecting the influence of the growing first resonance, for $S \lesssim 10^{-3}$. For $S \gtrsim 10^{-3}$, both the tunnel splittings and the overlaps start to grow exponentially, one by one, starting from the lowest doublet, so that the range of these quantities reduces by several orders of magnitude. The regime, on the S axis, of this steep increase coincides with that of the onset of chaotic motion in the classical dynamics. Insofar, the simple picture sketched in the Introduction is confirmed. Details of our expectation, however, need to be revised.

In particular, the notion that each splitting widens individually as the corresponding quantizing torus resolves, is not unambiguously corroborated by the data. It would imply that the transitions to a large splitting occur "from top to bottom", i.e., first for the doublet localized on the outermost torus pair within the separatrix. Indeed, if this transition is assessed from the splittings passing a certain absolute threshold, say $\Delta_\lambda = 10^{-4}$, that order is roughly obeyed. If, however, the point of onset of exponential growth, visible in a logarithmic plot like Fig. 5a, is taken as the criterion, the order is reversed.

Another remarkable fact is that the widening of the splittings and the concomitant change in character of the eigenstates, as functions of S, are continuous pro-

cesses that can only roughly be associated with the decay of a KAM torus, taken as a discrete event. Even doublet states overlapping by 70% with the chaotic layer may still show a relatively small splitting and exhibit the signature of a regular state in their spatial structure and time dependence (see Fig. 6). It remains to be clarified whether this retardation of the decay of the tunnel doublets corresponds to the gradual disintegration of classical tori via cantori and vague tori.

5. Driven tunneling with dissipation

In this section, we are going to extend our working model, Eq. (1), in such a way that it allows to describe the influence of dissipation and noise on the microscopic level. We follow the usual procedure of coupling the central system to a heat bath [44, 45], by adding two terms to the Hamiltonian (1), representing, respectively, the reservoir and its interaction with the double well,

$$H(t) = H_{\mathrm{DW}}(t) + H_{\mathrm{I}} + H_{\mathrm{R}}, \quad H_{\mathrm{I}} = \sum_i x(g_i b_i + g_i^* b_i^\dagger), \quad H_{\mathrm{R}} = \sum_i \omega_i (b_i^\dagger b_i + \frac{1}{2}). \quad (9)$$

Here, b_i, $b_i^\dagger$ are annihilation and creation operators, respectively, for a boson mode of frequency ω_i, and g_i is the corresponding coupling constant.

Proceeding in a similar way as in ref. [46], we use the density operator in the Floquet basis, reduced to the double-well degree of freedom, as the basis of our description, and resort to the usual rotating-wave and Markov approximations. This allows to derive the equation of motion for the density matrix $\tilde{\sigma}$ (in the interaction picture with respect to H_{I}), in the form of the master equation [46]

$$\dot{\tilde{\sigma}}_{\alpha,\beta}(t) = \delta_{\alpha,\beta} \sum_\nu \left(W_{\alpha,\nu}\tilde{\sigma}_{\nu,\nu}(t) - W_{\nu,\alpha}\tilde{\sigma}_{\alpha,\alpha}(t)\right) + \frac{1}{2}(1-\delta_{\alpha,\beta}) \sum_\nu \left(W_{\nu,\alpha} + W_{\nu,\beta}\right)\tilde{\sigma}_{\alpha,\beta}(t), \quad (10)$$

comprising a closed subset of equations for the approach of the diagonal elements towards a steady state, and another subset describing the decay of the non-diagonal elements. The coefficients $W_{\alpha,\beta}$ depend on the coupling constants and on the quasienergies; they are given elsewhere [17].

The classical limit of the quantal dynamics generated by Eq. (10) can be obtained, e.g., by switching from the density operator to a probability distribution in phase space, such as the Husimi distribution, and expanding with respect to $1/D$. Specifying the frequency dependence of the coupling strength as $|g(\omega)|^2 = \gamma\omega/\pi(1+\omega^2/\omega_{\mathrm{c}}^2)$, where ω_{c} is a cutoff frequency, we arrive at the Langevin equation [16, 17]

$$\ddot{x} + \gamma\omega_{\mathrm{c}} \int_{-\infty}^{t} \mathrm{d}t' \dot{x}(t') \exp\left(-\omega_{\mathrm{c}}(t-t')\right) - \frac{x}{2}(1 + 2\gamma\omega_{\mathrm{c}}) + \frac{x^3}{16D} + S\cos\omega t = f(t). \quad (11)$$

Here, $f(t)$ is a random force with the autocorrelation function $\langle f(t)f(t')\rangle = \gamma k_{\mathrm{B}} T \omega_{\mathrm{c}} \exp(-\omega_{\mathrm{c}}|t-t'|)$. Eq. (11) describes a bistable Duffing oscillator [6 - 9] with Ohmic damping and fluctuations.

The master equation (10) can now serve to investigate the influence of dissipation on the coherence effects characterizing driven tunneling, as discussed in Section 3

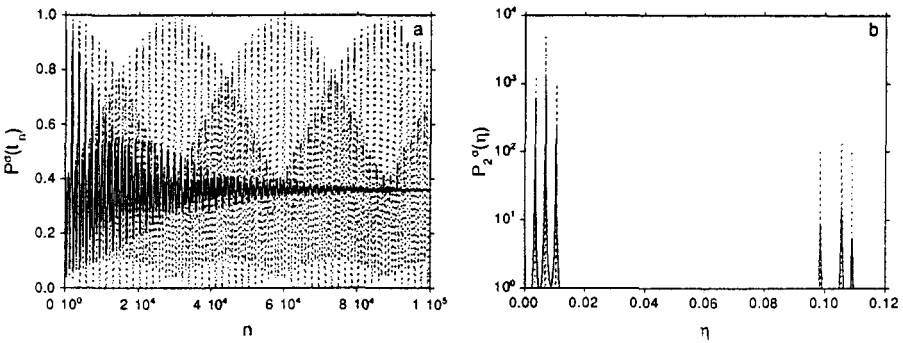

Fig. 7. Driven tunneling with dissipation. (a) Time evolution of $P^\sigma(t_n)$ over the first 2×10^5 time steps; (b) local spectral two-point correlation function $P_2^\sigma(\eta)$ as obtained from (a). The parameter values are as in the corresponding conservative case shown in Fig. 1 (repeated here in dashed lines), but with a finite damping constant, $\gamma = 4 \times 10^{-5}$, at zero temperature.

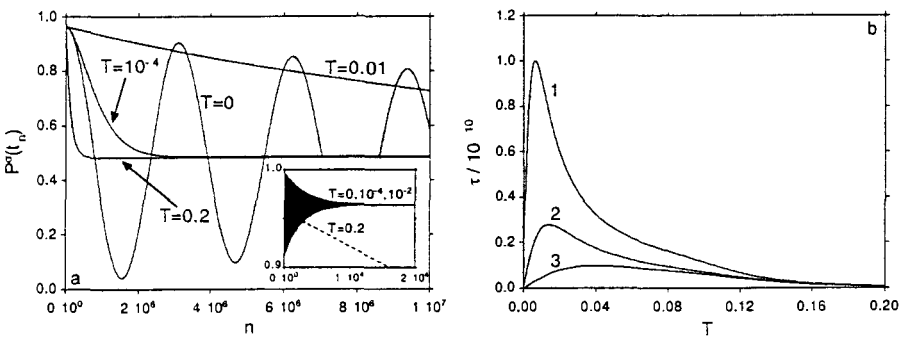

Fig. 8. Coherent suppression of tunneling in the presence of dissipation. (a) Time evolution of $P^\sigma(t_n)$ over the first 10^7 time steps, at a parameter point ($D = 2$, $\omega = 0.01$, and $S = 3.171 \times 10^{-3}$) close to $S_{\mathrm{loc},0}(\omega)$ (see Fig. 2a), for $\gamma = 10^{-6}$ and various values of T, starting from a pure, minimum-uncertainty state centered in one of the wells (inset: the first 2×10^4 time steps on an enlarged time scale); (b) temperature dependence of the decay time τ of $P^\sigma(t_n)$ for three values of the detuning $\Delta\omega$ from the manifold $S_{\mathrm{loc},0}(\omega)$ (graph 1: $\Delta\omega = -1.4 \times 10^{-7}$, as in part (a), 2: $\Delta\omega = 5.0 \times 10^{-7}$ at $S = 3.1712 \times 10^{-3}$, 3: $\Delta\omega = 1.4 \times 10^{-6}$ at $S = 3.1715 \times 10^{-3}$). The other parameters are as in part (a). The data shown do not extend down to $T = 0$, where $\tau(T)$ diverges, but start only with the rising part of this function.

[16, 17]. Fig. 7a shows the time evolution of $P^\sigma(t_n) = \mathrm{tr}[\sigma(t_n)\sigma(0)]$ (the analogue of $P^\Phi(t_n)$, see Eq. (6)) with an initial state $\sigma(0) = |\phi(0)\rangle\langle\phi(0)|$ and parameters of H_{DW} as in Fig. 1, but with a finite damping constant $\gamma = 4 \times 10^{-5}$, at zero temperature. The complex quantum beats characteristic of the corresponding conservative system (dashed line) die out and give way to a steady state with a finite constant value of $P^\sigma(t_n)$ (in a periodically driven system, the stationary state may still possess a time dependence, with the period of the driving, which however is invisible in a stroboscopic plot like this). The broadening of the quasienergy levels,

due to the incoherent transitions described by Eq. (10), can be read off the Fourier transform of $P^{\sigma}(t_n)$, Fig. 7b.

A particularly interesting question is whether the coherent suppression of tunneling observed in the conservative case (see Section 3), will survive in the presence of dissipation: In order to obtain an adequate description also of this phenomenon on basis of a master equation like Eq. (10), we have to avoid part of the rotating-wave approximation used in its derivation. This approximation is valid only if the time scales of the classical relaxation and of the conservative quantal dynamics are clearly separated. However, in the vicinity of the manifolds $S_{\mathrm{loc},k}(\omega)$ where the tunnel splitting vanishes (see Fig. 2a), exceedingly small energy scales and correspondingly large time scales occur in the undamped dynamics. This necessitates to take also quasienergy transitions into account that virtually violate energy conservation. Details of this refinement of the master equation are given in refs. [17, 47].

Fig. 8a shows the time evolution of the autocorrelation $P^{\sigma}(t_n)$ at a parameter point ($D = 2$, $\omega = 0.01$, $S = 3.171 \times 10^{-3}$) very close to, but not exactly on, $S_{\mathrm{loc},0}(\omega)$, for $\gamma = 10^{-6}$ and various values of T. For low temperature, $P^{\sigma}(t_n)$ exhibits a slowly decaying coherent oscillation with a very long period, due to the slight offset from $S_{\mathrm{loc},0}(\omega)$. Also here, there exist superposed oscillations reflecting the admixture of other quasienergy states. Their decay is visible only on an enlarged time scale (inset in Fig. 8a). Asymptotically, the distribution among the wells is completely thermalized. With increasing temperature, the decay time of the slow coherent oscillation first decreases until this oscillation is suppressed from the beginning (the corresponding part of the graph is not shown in Fig. 8b). After going through a minimum, however, the thermalization time increases again. At a characteristic temperature T^{*}, this time scale reaches a resonance-like *maximum* where the incoherent processes induced by the reservoir *stabilize* the localization of the wave packet in one of the wells and thus compensate for the detuning introduced deliberately. In Fig. 8b, we present the temperature dependence of the decay time τ (defined by $P^{\sigma}(t_n) \sim \exp(-n/\tau)$) for three values of the detuning $\Delta\omega$ from the manifold $S_{\mathrm{loc},0}(\omega)$: With increasing $\Delta\omega$, the maximum is shifted towards higher temperatures and decreases in height. A variation of γ reveals that there exists a similar, resonance-like dependence also on the damping constant [47].

We emphasize that this stabilization of the coherent suppression of tunneling by noise is distinct from the trivial localization by strong damping. In fact, it has already been observed in a model simpler than the present one, where the deterministic harmonic driving of the double well was replaced by a noisy one, so that the time evolution remained unitary and a damping could not occur [12]. Rather, this phenomenon bears some resemblance to the quantum Zeno effect in a bistable system [48], and to the classical stabilization of instable equilibrium states by multiplicative noise [49, 50].

Up to now, we discussed the influence of dissipation on coherence effects. Conversely, one may also ask how the classical dynamics of the driven damped Duffing oscillator [6 – 9] is modified by quantal interference. A hallmark of the classical dynamics is the existence of attractors of various degrees of complexity, as a function of ω, S, or γ. In Figs. 9, 10 [47], we choose parameter values ($D = 6$, $S = 0.0849$, $\omega = 0.9$, $\gamma = 10^{-5}$, and $T = 0$) where classically, there exist five limit cycles, with

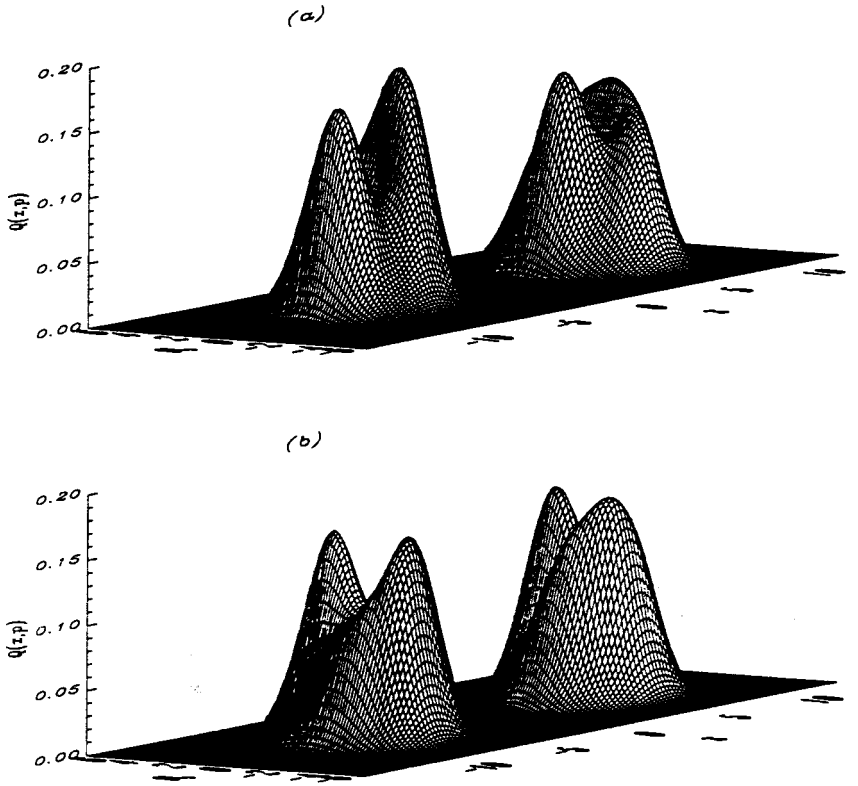

Fig. 9. Quantal stationary state. Asymptotic Husimi distribution at $D = 6$, $S = 0.0849$, $\omega = 0.9$, $\gamma = 10^{-5}$, and $T = 0$, at phases (a) 0 and (b) $\pi/2$.

the frequency of the driving: two symmetry-related pairs with one partner within each well, and a single one encircling the wells. Fig. 9 shows the Husimi distribution in the stationary state at phases (a) 0 and (b) $\pi/2$. The broadening by quantal noise, compared to the corresponding classical, delta-like asymptotic distributions is obvious. In Fig. 10, we compare the distributions of Fig. 9a to the phase-space portrait of the corresponding conservative classical system. Both the classical attractors and the maxima of the quantal stationary distribution, while not coinciding exactly, are located near elliptic fixed points of the conservative dynamics and can be associated with the regular regions around the potential minima and the first resonance, respectively (the fifth limit cycle outside the wells is not significantly populated in the quantal stationary state). Furthermore, we see that the quantum noise preferentially broadens the stationary distribution along the limit cycle to which the corresponding

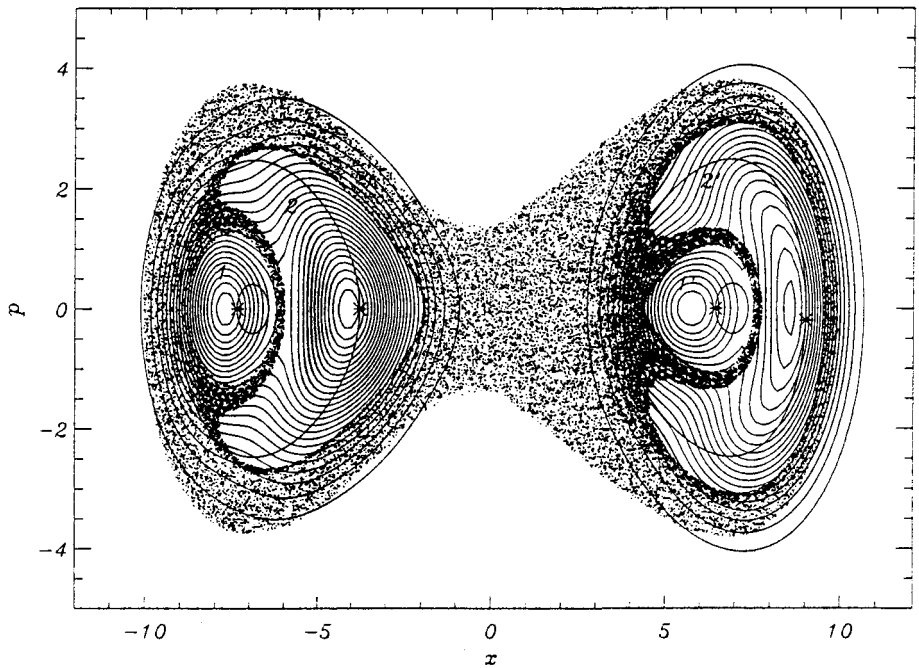

Fig. 10. Quantal stationary state. Contour plot of the asymptotic Husimi distribution at $D = 6$, $S = 0.0849$, $\omega = 0.9$, $\gamma = 10^{-5}$, and $T = 0$, compared to the limit cycles of the corresponding classical system (the positions on the cycles at phase 0 are indicated by asteriscs), and to the phase-space portrait of the corresponding conservative dynamics.

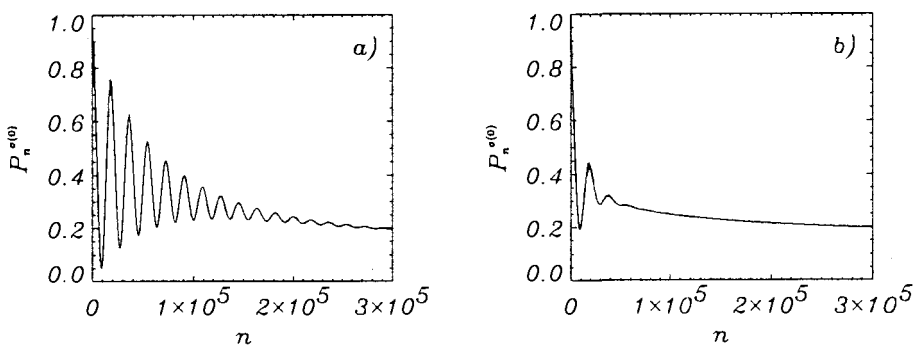

Fig. 11. Transient tunneling between limit cycles. (a) Time evolution of $P^{\sigma}(t_n)$ over the first 3×10^5 time steps, at paramater values as in Figs. 9, 10, but with $\gamma = 5 \times 10^{-6}$, for initial states prepared as coherent states located at either one of the maxima of the stationary Husimi distribution in the left well, i.e., at $p = 0$ and (a) $x = -7.5$, (b) $x = -4.2$.

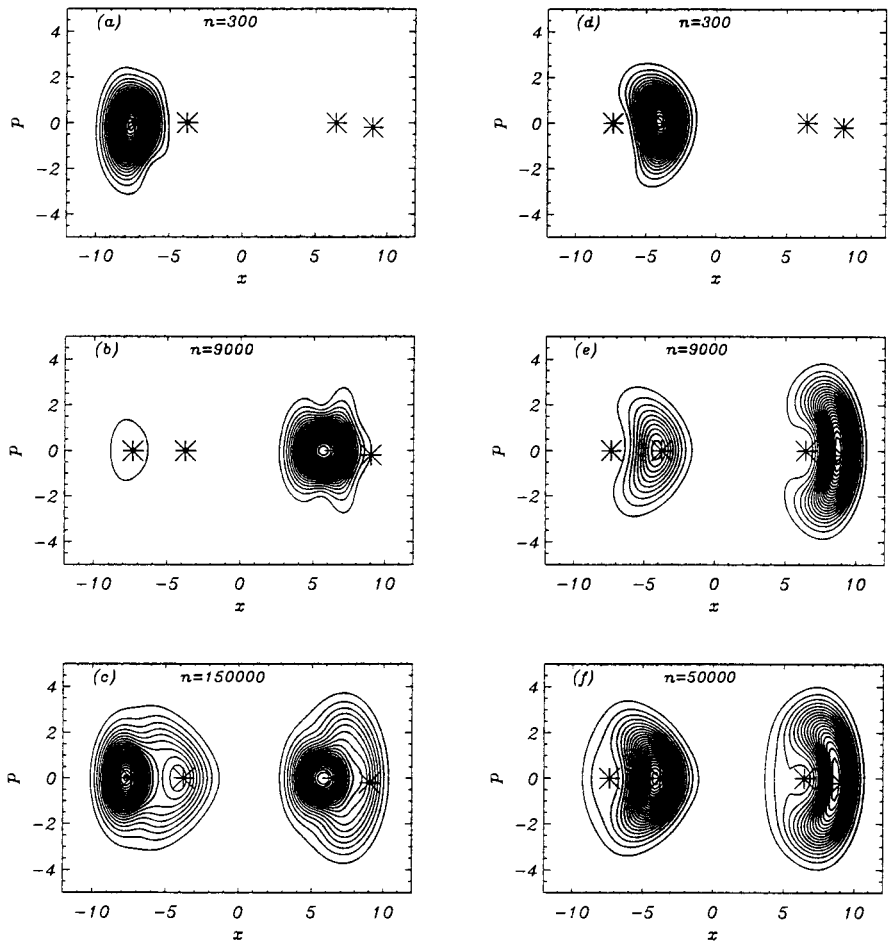

Fig. 12. Transient tunneling between limit cycles. Husimi distribution at various times, for initial states prepared as coherent states located at either one of the maxima of the stationary Husimi distribution in the left well, i.e. at $p = 0$ and (a - c) $x = -7.5$, (d - f) $x = -4.2$. The positions, at phase 0, on the limit cycles of the corresponding classical dynamics are indicated by asteriscs.

classical attractor belongs. This is the direction in which the classical phase-space flow is least contractive [51].

While the smoothing due to quantum noise is the only quantum effect left in the stationary state, a remnant of coherent tunneling survives in the transient behavior [47]. Fig. 11 shows the time evolution of $P^{\sigma}(t_n)$ for the same parameter values as

above, with the initial states prepared as coherent states at the location of either one of the maxima of the asymptotic distribution (see Fig. 10) within the left well, corresponding to nonresonant motion (a) and to the first resonance (b), respectively. In both cases, we observe a coherent oscillation decaying as the stationary state is approached. Fig. 12 reveals that these oscillations indeed form a remnant of tunneling within each the symmetry-related pairs of regular regions. The stationary distribution among both pairs is reached only on the longer time scale of the classical relaxation. Clearly, we here observe tunneling between limit cycles.

6. Summary

The present paper is intended to highlight a number of facettes of the nonlinear dynamics in a periodically driven double-well potential, at different stages of the transition from microscopic, coherent to macroscopic, incoherent behavior. Our main tool has been a numerical analysis on basis of the Floquet formalism, which allows to speak of quasienergies and quasienergy eigenstates of the driven system, in analogy to eigenenergies and eigenstates in the undriven case.

In the deep quantal regime, we find modifications, due to the driving, of the familiar tunneling. They range from a mere acceleration of its rate, in the two extremes of slow and of fast driving, through complex quantum beats near resonances with the unperturbed system frequencies, to an almost complete suppression of tunneling by a coherent mechanism effective along one-dimensional manifolds in the parameter space spanned by amplitude and frequency of the driving.

Towards the semiclassical limit of the conservative system, the quantal behavior begins to exhibit clear traces of the classical dynamics. Specifically, we addressed the interplay between coherent transport by tunneling and diffusive transport along the chaotic layer developing in the vicinity of the separatrix of the undriven system. Eigenstate doublets residing within the paired, symmetry-related regular regions of the classical phase space exhibit exponentially small splittings and thus support tunneling. As the pair of quantizing tori pertaining to such a doublet resolves in the chaotic sea, the splitting widens and tunneling gives way to a more complex dynamics contributing to the quantal counterpart of chaotic diffusion. On a closer look, however, the scenario turns out to be less simple. For example, classical tori disintegrate only via intermediate steps, dubbed "cantori" and "vague tori", with the consequence that the transition from a regular to a chaotic nature of a quasienergy eigenstate is not sharply defined, but rather proceeds in a smooth and retarded manner. Accordingly, a strict distinction between regular and chaotic regions is inadequate on the quantum-mechanical level.

The other principal ingredient of the crossover to macroscopic behavior, besides a small relative $\hbar$, is the coherence-disturbing effect of the ambient degrees of freedom, modelled microscopically as a coupling to a quasicontinuous reservoir. As an immediate consequence, the incoherent processes render the coherence effects observed in the deep quantal regime transients. Surprisingly, however, the coherent suppression of tunneling is stabilized if damping constant and reservoir temperature are in a specific regime, a result akin to the quantum zeno effect and to the classical stabilization of instable equilibria by multiplicative noise. On the time scale of classical

relaxation, the dissipative quantum dynamics approaches a stationary state which forms the analogue of the attractors of the corresponding classical dynamics. The most conspicuous quantum effect left in these stationary states is a broadening due to quantum noise. It is not isotropic, but acts preferentially in the direction where the classical phase-space flow is least contractive, that is for example, stronger along limit cycles than transverse to them.

Quite a number of questions have been left open. In the conservative case, they concern, e.g., an analytical description, in terms of semiclassical concepts, of tunneling in the presence of chaos. In the parameter regime of the dissipative system where several strange attractors coexist, both transient tunneling between their basins of attraction, and the quantal smoothing of the fractal basin boundaries [52] could be addressed. Finally, it should be checked whether the phenomenon of stochastic resonance, generated by external classical noise in periodically driven bistable systems [53], can be induced by the inherent quantum noise as well.

7. Acknowledgement

One of us (BO) acknowledges financial support by the Free State of Bavaria.

References

1. S. Chakravarty and S. Kivelson, Phys. Rev. Lett. **50**, 1811 (1983).
2. M. H. Devoret, D. Estéve, J. M. Martinis, A. Cleland, and J. Clarke, Phys. Rev. B **36**, 58 (1987); J. Clarke, A. N. Cleland, M. H. Devoret, D. Estéve, and J. M. Martinis, Science **239**, 992 (1988).
3. R. Bavli and H. Metiu, Phys. Rev. Lett. **69**, 1986 (1992).
4. J. E. Combariza, B. Just, J. Manz, and G. K. Paramonov, J. Phys. Chem. **95**, 10351 (1992).
5. L. M. Sander and H. B. Shore, Phys. Rev. B **3**, 1472 (1969).
6. P. Holmes, Philos. Trans. R. Soc. London, Ser. A **292**, 419 (1979).
7. B. A. Huberman and J. P. Crutchfield, Phys. Rev. Lett. **43**, 1743 (1979).
8. Y. Ueda, J. Stat. Phys. **20**, 181 (1979); Ann. N. Y. Acad. Sci. **357**, 422 (1980).
9. W. Szemplińska-Stupnicka, Nonlinear Dynamics **3**, 225 (1992).
10. F. Hund, Z. Phys. **43**, 803 (1927).
11. F. Grossmann, P. Jung, T. Dittrich, and P. Hänggi, Z. Phys. B **84**, 315 (1991); Phys. Rev. Lett. **67**, 516 (1991).
12. F. Grossmann, T. Dittrich, P. Jung, and P. Hänggi, J. Stat. Phys. **70**, 229 (1993).
13. F. Grossmann, T. Dittrich, and P. Hänggi, Physica B **175**, 293 (1991).
14. T. Dittrich, F. Grossmann, P. Jung, B. Oelschlägel, and P. Hänggi, Physica A **194**, 173 (1993).
15. F. Grossmann and P. Hänggi, Europhys. Lett. **18**, 571 (1992).
16. T. Dittrich, B. Oelschlägel, and P. Hänggi, Europhys. Lett. **22**, 5 (1993).
17. B. Oelschlägel, T. Dittrich, and P. Hänggi, Act. Phys. Pol. B **24**, 845 (1991).
18. R. Utermann, T. Dittrich, and P. Hänggi, in *Proceedings of the XXth International Conference on Low Temperature Physics, Eugene, 1993*, edited by R. J. Donnelly (North-Holland - Elsevier, Amsterdam, 1993).
19. R. Utermann, T. Dittrich, and P. Hänggi, submitted to Phys. Rev. E.
20. J. H. Shirley, Phys. Rev. **138B**, 979 (1965).
21. H. Sambe, Phys. Rev. A **7**, 2203 (1973).
22. N. L. Manakov, V. D. Ovsiannikov, and L. P. Rapoport, Phys. Rep. **141**, 319 (1986).
23. S. Chu, Adv. Chem. Phys. **73**, 739 (1989).
24. A. Peres, Phys. Rev. Lett. **67**, 158 (1991).
25. P. W. Anderson, Phys. Rev. **109**, 1492 (1958); Rev. Mod. Phys. **50**, 191 (1978).
26. D. R. Grempel, R. E. Prange, and S. Fishman, Phys. Rev. A **29**, 1639 (1984).
27. J. von Neumann and E. Wigner, Phys. Z. **30**, 467 (1929).

28. M. V. Berry, in *Chaotic Behavior in Quantum Systems: Theory and Applications*, edited by G. Casati, vol. 120 of *NATO ASI Series B: Physics* (Plenum, New York, 1985).
29. J. M. Gomez Llorente and J. Plata, Phys. Rev. A **45**, R6958 (1992).
30. L. E. Reichl and W. M. Zheng, in *Directions in Chaos, vol.1*, edited by H. B. Lin (World Scientific, Singapore, 1987), p. 17.
31. A. J. Lichtenberg and M. A. Lieberman, *Regular and Stochastic Motion*, Vol. 38 of *Appl. Math. Sci.* (Springer, New York, 1983).
32. M. J. Davis and E. J. Heller, J. Chem. Phys. **75**, 246 (1986).
33. O. Bohigas, S. Tomsovic, and D. Ullmo, Phys. Rev. Lett. **64**, 1479 (1990); *ibid.* **65**, 5 (1990).
34. S. Tomsovic and D. Ullmo, *Tunneling in the Presence of Chaos*, preprint, 1990.
35. O. Bohigas, S. Tomsovic, and D. Ullmo, Phys. Rep. **223**, 43 (1993).
36. W. A. Lin and L. E. Ballentine, Phys. Rev. Lett. **65**, 2927 (1990); Phys. Rev. A **45**, 3637 (1992).
37. J. Plata and J. M. Gomez Llorente, J. Phys. A **25**, L303 (1992).
38. H. P. Breuer and M. Holthaus, Ann. Phys. (N. Y.) **211**, 249 (1991).
39. M. V. Berry and M. Robnik, J. Phys. A **17**, 2413 (1984).
40. L. E. Reichl, in *The Transition to Chaos: In Conservative and Classical Systems: Quantum Manifestations* (Springer, New York, 1992), Chaps. 3.9, 9.5.1, and refs. therein.
41. W. P. Reinhardt, J. Phys. Chem. **86**, 2158 (1982); R. B. Shirts and W. P. Reinhardt, J. Chem. Phys. **77**, 5204 (1982).
42. K. Husimi, Proc. Phys. Math. Soc. Jap. **22**, 264 (1940).
43. R. J. Glauber, in *Quantum Optics*, edited by A. Maitland (Academic, London, 1970).
44. H. Haken, vol. XXV/2c of *Encyclopedia of Physics*, edited by S. Flügge (Springer, Berlin, 1970).
45. W. H. Louisell, *Quantum Statistical Properties of Radiation* (Wiley, London, 1973).
46. R. Blümel, A. Buchleitner, R. Graham, L. Sirko, U. Smilansky, and H. Walther, Phys. Rev. A **44**, 4521 (1991).
47. B. Oelschlägel, Ph. D. thesis, University of Augsburg, unpublished (1993).
48. M. J. Gagen, H. M. Wiseman, and G. J. Milburn, Phys. Rev. A **48**, 132 (1993).
49. R. Graham and A. Schenzle, Phys. Rev. A **26**, 1676 (1982).
50. M. Lücke and F. Schank, Phys. Rev. Lett. **54**, 1465 (1985).
51. T. Dittrich and R. Graham, Europhys. Lett. **4**, 263 (1987); Ann. Phys. (N. Y.) **200**, 363 (1990).
52. C. Grebogi, S. W. McDonald, E. Ott, and J. A. Yorke, Physics Letters **99A**, 415 (1983); S. W. McDonald, C. Grebogi, E. Ott, and J. A. Yorke, Physica D **17**, 125 (1985).
53. F. Moss, Ber. Bunsenges. Phys. Chem. **95**, 303 (1991), and refs. therein.